N 1/4*

Japanese Contributions to Structural, Mechanical and Stress Analysis of INTOR

S. Nishio
Japan Atomic Energy Research Institute, Naka-machi, Naka-gun, Ibaraki-ken 311-02, Japan
T. Honda, Y. Sawada
Toshiba Corporation, Tokyo, Japan

The present phase (named Phase-IIA) of the International Tokamak Reactor (INTOR) study has been set up to critically address issues which affect the feasibility, cost, and engineering simplicity of the concept. The main objective of the study was to produce a new design concept with a significant reduction in the size of the tokamak device while maintaining the plasma size and performance. This paper highlights major design features and structural, mechanical and stress analysis of the Japanese INTOR Phase-IIA (INTOR J-IIA) concept.

Critical issues identified at the beginning of Phase-IIA INTOR Workshop have been consistently investigated through design activities of INTOR J-IIA which is modification of INTOR Phase-One concept. The INTOR J-IIA has the following principal features. The bore of the toroidal field coil is reduced from 7.7 m wide × 10.7 m high for phase I reference design to 6.6 m wide × 9.3 m high. The poloidal field coil distribution for pumped limiter operation is selected. The torus structures of both limiter and blanket are divided into 24 sectors. Each of two sectors between two TF coils is retracted in radial direction with different angle.

The effort of structural and stress analysis was mainly focused on first wall and pumped limiter as well as superconducting magnets, because first wall and pumped limiter are to receive most servere heat load from a burning plasma, and the magnet system is exposed to enormous electromagnetic loading. Furthermore, seisimic analysis was carried out to ensure that the reactor structure is designed to meet the criteria imposed by the design basis earthquakes. As the calculated results, each maximum stress intensity in main components is allowable according to ASME code.

The INTOR J-IIA configuration is not necessarily optimized yet for total system; however, the solution developed has been useful in this conceptual design pahse to design and evaluate the many component associated with a tokamak reactor.

1. Introduction

The broad tasks of the Zero-Phase INTOR Workshop which was conducted during 1979 were to define the objectives and physical characteristics of the next major experiment (after JT-60, TFTR, JET, T-15), in the world-wide tokamak programme and to assess the technical feasibility of constructing this experiment. Detailed assessments of the plasma physics and technology bases for such an INTOR experiment were developed, and physical characteristics were identified /1/. On the basis of the Zero-Phase studies, the INTOR Workshop was extended into Phase-One which was conducted from 1980 to 1981. The objective of the Phase-One Workshop was to develop a conceptual design of INTOR experiment. The starting point for the conceptual design effort was the set of reference parameters suggested by the Zero-Phase Workshop. The conceptual design in the Phase-One INTOR Workshop had been published /2/.

After the Phase-One, the INTOR Workshop had come into next stage named Phase-IIA. During the Phase-IIA INTOR Workshop (July 1981 to the end of 1982), the emphasis had been upon addressing critical technical issues which affect the feasibility, cost and engineering design simplicity of the concept. The major design requirements established to meet the previous emphasis are (1) minimization of the TF coils and the reactor size under the condition of the remote maintenance and the field ripple less than 1.2%, (2) adoption of pumped limiter for density and impurity control (in Phase-One conceptual design, a poloidal divertor was employed), (3) adoption of RF heating instead of NBI heating and (4) use of 12 TF coils as in Phase-One.

In Chapter 2, the design features of Japanese INTOR Phase-IIA concept (in short, INTOR J-IIA) are described. In chapter 3, the structure and stress analysis including the seismic analysis are described. And in the last chapter, the conclusions and the recommendations for further work are described.

2. Design Features of INTOR J-IIA

Critical issues identified at the beginning of Phase-IIA of INTOR Workshop have been consistently investigated through design activities of INTOR J-IIA, which is modification of Japanese version of INTOR Phase-One activity (INTOR J /3/). As a results of new concepts developed during Phase-IIA, a smaller INTOR J-IIA configuration shown in Fig. 1 has evolved which is reflected in the radial build drawings shown in Fig. 2. The principal engineering parameters are given in Table 1.

2.1 Torus System

Segmentation

Five representative options mentioned were considered from the viewpoint of relations between the number of torus segmentation and the replacement procedures. These five are (a) one sector/TF coil with straight radial motion (as Phase-One), (b) two sectors/TF coil with straight oblique motion,(c) two sectors/TF coil with two motions (oblique and radial), (d) three sectors/TF coil with single straight motion (radial or oblique) and (e) three sectors/TF coil with two motion (rotation in toroidal direction and straight radial motion).

The option (b) as shown in Fig. 3 is selected as our recommended option. The advantage of this concept is that the retraction motion is single straight motion which is relatively simple and highly reliable. Though two sections/TF coil should be retracted in two different direction respectively, this concept permits a reduction of TF coil bore size with obtaining a sufficiently thick coil case. In order to avoid the T shaped vacuum seal which seems to be less reliable, a blanket access door for the separate vacuum closure is provided on the blanket access port shown in Fig. 3.

Vacuum topology

There are several concept /4/ for separate and combined vacuum boundaries for the torus and superconducting magnet vacuum system. The choice of the vacuum boundary configuration should be made according the consideration taken for the vacuum boundary technical issues such as; (1) safety, (2) reliability, (3) maintenability, (4) producibility and cost, (5) torus one turn resistance, (6) penetration and accessibility, (7) influence by bake out and (8) influence of electromagnetic force.

The simplified separate vacuum boundary is selected in our new design, as shown in Fig.4. In this concept, there are no problem concerning the thermal displacement at torus bake-out and no propagation of accident because the plasma vacuum boundary and the cryostat are independent. The simgle bellow for the plasma chamber is selected in order to economize the space for shield structure.

2.2 Pumped Limiter

As shown in Fig. 1 and Fig. 5, the pumped limiter is located at the bottom of the reactor core because of better tritium breeding ratio in the blanket, better conductance for pumping and possibility of the poloidal divertor option. The shape of limiter plate is the curved double-edged limiter from the viewpoint of the heat flux on the limiter plate and the particle pumping speed.

The pumped limiter is segmented as two sectors/TF coil because of insufficient space for retracting one sector limiter and fixed into the blanket sector as shown in Fig. 5 and Fig. 6. The pumped limiter between two adjacent TF coils consists of a large sector and a small sector which are to be retracted horizontally in radial direction. For the torus vacuum boundary, the limiter access door is equipped on the blanket access door. The cooling pipes coming from each limiter sector pass through the access door on which the vacuum sealing is carried out.

The pumped limiter is composed of a surface armor, cooling plate and structure reinforcement. Pyrolytic graphite (PG) as an armor material is employed for reference design through the investigation of several candidate materials /5/. The materials for cooling palte and structure reinforcement are 0.2% Ag OFCu and type 316 stainless steel as shown in Fig. 7. A surface armor and cooling plate are connected by brazing method.

2.3 Magnet System

Toroidal field (TF) coil

The major requirement for the INTOR TF magnet is to provide total ampereturns of 143 MAT requried to generate the 5.5 T field at plasma major radius of 5.2 m. the overall current density in the winding of TF magnet is 19.4 A/mm^2 and the maximum field is 11.4 T at the magnet bore. The pool boiling method is adopted and fulfils the cryogenic stabilization. The magnet is graded at three fields: These are 12T, 10T and 5T field respectively. The conductors of 12T and 10T consist of the conductor of copper stabilized Nb_3Sn. The conductor of 5T consists of copper stabilized NbTi conductor.

The AC loss is caused by the changing poloidal field mainly at the superconductor, the helium vessel and the coil support in the TF coils. For the pumped limiter operation, the average AC loss is 56 kW.

Poloidal field (PF) coil

The optimization of PF coil location and ampere turn are carried out on the basis of the following four principle points;

(1) relevancy with the reactor structure system,

(2) reduction of power capacity of electrical supply,

(3) strength of TF coil structure,

(4) reduction of AC loss in superconducting conductor and coil case structure induced by pulsed magnetic field.

The selected PF coil location is shown in Fig. 1. The outer-most block diamter is 11 m and maximum total magneto-motive force is 83.5 MAT. The Motor-Generator peak power is 0.9 GW in comparison to 3.1 GW of the Phase-One design.

A pool boiling system is employed mainly because of efficient cooling and matured technology. Three composite superconducting material composed of NbTi, copper and CuNi is used for the achievement of low AC losses. The maximum field is 7.1T and the average AC loss of all PF coils amounts to 3.8 kW.

3. Structural and Stress Analysis

Analytical work description is mainly focused on first wall and pumped limiter as well as superconducting magnets, because first wall and pumped limiter are to receive most severe heat load from the burning plasma, and the magnet system is exposed to enormous electromagnetic loading.

3.1 First Wall

Table 2 and Fig. 8 show the operating condition and mechanical configuration of the first wall respectively. First wall is made of stainless steel. Highest temperature at wall surface is approximately 273°C, and maximum thermal stress is approximately 220 MPa, taking account of stress concentration at groove bottoms, which clearly satisfies the limit of 3 Sm based on ASME. In addition to the normal operating condition, first wall behaviour against plasma disruptions was studied. Considering the heat load of 175 J/cm^2 for 20 ms and shielding effect by vaporized wall material, melt layer thickness is 0.014 mm for every disruption. Surface tension force acting on the melt layer was found to be larger than resultant force of gravity and electromagnetic force. Calculation result shows the vaporization of the first wall during the plasma disruption can be neglected from the stand point of life estimation. Therefore loss of first wall surface material during plasma disruptions could be neglected. Some experimental work will be needed to verify the above-mentioned analysis on the first wall dynamic behaviour.

3.2 Pumped Limiter

Table 3 and Figs. 5, 7 show the operating condition and mechanical configuration of the pumped limiter respectively. Two dimensional temperature calculation shows that maximum temperature at the armor surface is about 210°C with maximum heat load of 2.1 MW/m^2 and temperature at leading edge is about 200°C. Thermal stress in the armor, the copper heat sink and the stainless steel reinforcement are 25, 47 and 44 MPa respectively which satisfy the limit of 3 Sm based on ASME Section III. There is much uncertainty about irradiation effect on material properties, and a lot of research will be required in this field. Thermal analysis about dynamic behavior during plasma disruption shows that no remarkable melting occurs in the armor material. Concerning the sputtering problem, sputtering yields were summed up for several dominant ion components such as D^+, T^+, He^+ and so forth. Neglecting redeposition of the armor material, approximately 12.5 mm of the armor will be ablated every year during the operation. However, if 80% redeposition is assumed, sputtering will be reduced to 2.5 mm a year and a life of more than 40 months can be expected.

The mechanical stress caused by plasma disruption is 0.8 S_m (Cu: 0.8 S_m = 31 MPa, stainless steel: 0.8 S_m = 108 MPa) and is allowable according to the ASME Sec. III.

3.3 TF Coil

Electromagnetic forces acting on the TF coils are as follows.

Hoop force		1144 MN/coil
Centering force		379 MN/coil
Out of plane force (See Fig. 9)	M_x	213 MN-m/coil
	M_z	±239 MN-m/coil

The centering force acting on the TF coils is to be mainly taken by the wedge-action between the nose parts of the TF coils, though some fraction of the total force will be taken by the shear panels between the TF coils. The nose part of the helium vessel is designed to be fairly thick, approximately 300 mm thick, to withstand compression force due to the centering force.

Mechanical stress due to the above mentioned forces were calcualted based on three dimensional finite element method (FEM). In addition to the FEM analysis, local bending stress in the helium vessel, caused by the over-turning moment, was also calculated. Table 4 shows resultant mechanical and allowable stresses based on ASME code. It is clear that the calculated stress values satisfy the evaluation standard of ASME.

3.4 PF Coil

Electromagnetic force acting on PF coils consists of hoop force and bending moment caused by interaction among PF coil blocks. Two dimensional axisymmetric stress analysis was carried out and calculation model is shown in Fig. 10 . It is assumed that superconductors cannot contribute to the mechanical rigidity of winding structure and only stainless steel reinforcement takes the hoop force. The calculation result of stress distribution in radial direction is shown in Fig. 11 . The maximum stress intensity of reinforcement is 277 MPa and is allowable according to Table 4. The equivalent maximum cyclic stress ampitude S_{eq} is 160 MPa and given by the following formula.

$$S_{eq} = \frac{S_{alt}}{1 - \frac{S_{mean}}{S_u}}$$

S_{alt} : Cyclic stress amplitude

S_{mean}: Modified mean stress

S_u : Ultimate strength

This S_{eq} is below the design fatigue stress of 310 MPa for 10^6 cycles. The out-of-plane force is assumed to be supported by stainless steel support structure attached to helium vessel of FRP, because the bending stiffness of conductor and stainless steel tape inserted between turns is felt to be small. The bending stresses of 50 mm thick support structure are about 50 MPa in the outer-most ring coil. This stress is below the allowable stress according to Table 4.

3.5 Seismic Analysis

Seismic Analysis has been carried out to ensure that the reactor structure is designed to meet the criteria imposed by the design basis earthquakes. A great number of degree of freedom is required for dynamic analysis of the three-dimensional model of the system under consideration such as soil-reactor building-reactor structure system. So, in order to reduce significantly soil-reactor building system and the reactor structure system (including TF coils and blanket/shield torus) are analyzed separately: the former is analyzed with

rocking-sway model, the latter with the three dimensional FEM model.

The basic design earthquakes are S_1 (maximum possible earthquake, magnitude 8.4, epicentral distance 90 km) and S_2 (maximum credible two types of seismic waves; magnitude 7.5, epicentral distance 24 km and magnitude 8.5, epicentral distance 68 km). As for roch type, the soft rock is adopted (shearing wave speed V_s = 500 m/s). The natural frequency for both TF coil system and Blanket/shield torus system are shown in Table 5. The maximum stresses appearing in the main parts of the systems are shown in Table 6. Judging from these results, both TF coil system and Blanket/sield torus system are able to withstand the design basis earthquakes.

4. Conclusions and Recommendations

Design features of Japanese version of INTOR and associated analyses are summarized in the previous chapters. As a result of our new concepts developed during the Phase-IIA, the reactor has become less expensive and smaller than the reference INTOR Phase-One design with retaining the plasma size and performance parameters. As progress has been made in generating further design and analytical detail in many areas, our understanding of the components and the technical feasibility of the overall device might be advanced.

However, further experimental works connected with irradiation effect on the first wall and the pumped limiter structure material must be carried out. It is also very important to investigate in detail the dynamic behaviour of the first wall and the pumped limiter, such as sputtering problems and melt layer performance during plasma disruption. As for the magnet system, further intensive efforts should be made to ensure mechanical integrity of the magnet structure, including superconducting windings, helium vessel, supporting structures and interface technology to get those structures rigidly connected with each other.

ACKNOWLEDGEMENT

The authers would like to thank Drs. F. Farfaletti-Casali (Joint Research Center, Ispra Establishment, Italy), T.G. Brown (Fusion Engineering Design Center, Oak Ridge, USA), G. Churakov (D.V. Efremov Scientific Institute, Leningrad, USSR), P. Reynolds (Culham Laboratory, United Kingodm), D. Serebrennikov (D.V. Efremov Scientific Institute, Leningrad, USSR), T.E. Shannon (Fusion Engineering Design Center, Oak Ridge, USA) for their fruitful discussions and comments. It is our pleasure to thank Drs. T. Hiraoka, K. Tomabechi and S. Mori for their continuous encouragements throughout this work.

REFERENCE

/1/ INTOR Zero Phase, IAEA, Vienna, 1980

/2/ INTOR Phase-One, IAEA, Vienna, 1982

/3/ Y. Sawada, et al., Third IAEA Technical committee Meeting and Workshp on Fusion Reactor Design and Technology, 5-16 Oct. 1981, Tokyo

/4/ S. Nishio, et al., JAERI-M 82-178, Nov. 1982

/5/ T. Hiraoka, et al., JAERI-M 82-174, Nov. 1982

Table 1 Principal INTOR engineering parameters

	Phase One	J-II A
Thermonuclear power, MW	620	
Plasma major radius, m	5.3	
Plasma minor radius, m	1.2	
Plasma elongation	1.6	
Plasma current, MA	6.4	
Toroidal field on axis, T	5.5	
Number of TF coils	12	
TF coil bore size, m	7.7 × 10.7	6.6 × 9.3
PF stored energy, GJ	15.3	4.3
Impurity control	single-null divertor	pumped limiter
Plasma heating system	NBI	ICRH

Table 2 First wall operating condition

Total plasma chamber area	380 m^2
Average neutron wall laoding	1.3 MW/m^2
Radiative power from plasma	40 MW
Average nuclear heating	12 W/cm^3
Neat load during disruption	175 J/cm^2 (for 20 ms)

Table 3 Operating condition for pumped limiter

Item	Description	
Operating condition	Edge temperature	150 eV
	Total energy to pumped limiter	60 MW
	Plasma disruption energy	270 J/cm^2 for 20 mS
	Total particle flux to limiter	$1.25 \times 10^{24}/cm^2 \cdot s$

Table 5 Natural frequency (Hz)

Mode	Blanket/Shield torus	TF coils
1	14.95	7.06
2	15.12	8.06

Table 4 Allowable stress and maximum stress intensities of TF coil

Part		Materials	Ultimate strength σ_u (MPa)	Yield strength σ_y (MPa)	Sm (MPa)	Maximum stress intensities (MPa)	
						P_m (< Sm)	$P_L + P_b$ (< 1.5 Sm)
Helium vessel		SUS316L	1,580	670	440	395	485
Winding	Stainless steel reinforcement						
	Copper stabilizer	OFHC$\frac{1}{2}$ H	440	330	220	161	221

P_m: membrance stress, P_L: local membrance stress, P_b: bending stress

Table 6 Maximum stress (MPa)

Design wave	S_1	S_2
Torus support (axial stress)	3	10
TF coil structure (bending stress)	23	38
TF coil support (bending stress)	49	81

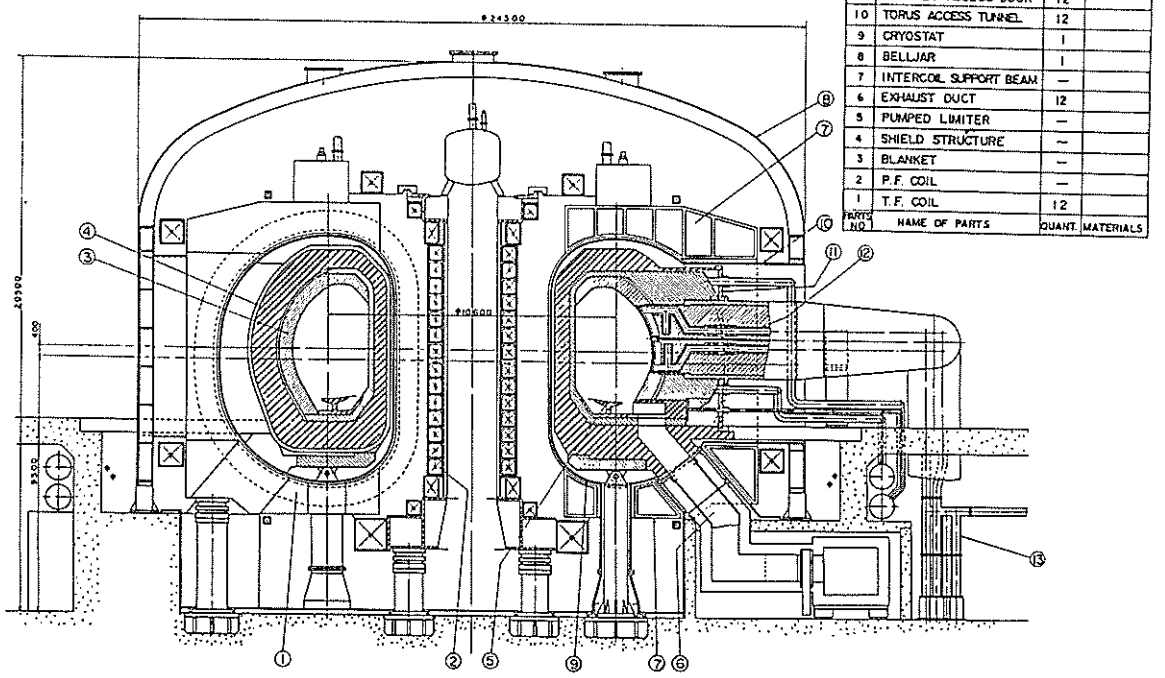

Fig.1 INTOR-J-IIA Vertical view of INTOR

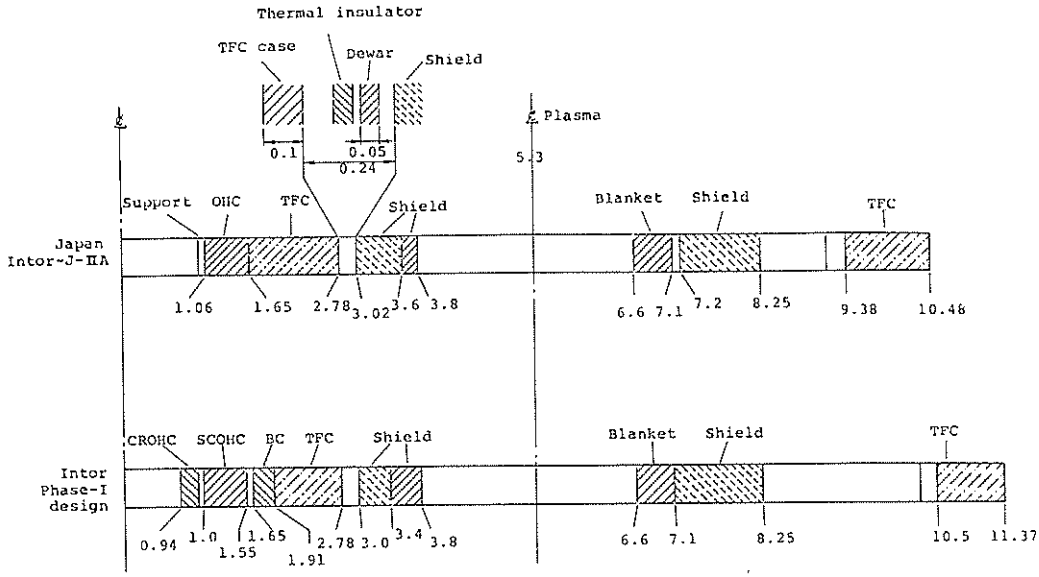

Fig. 2 Radial build

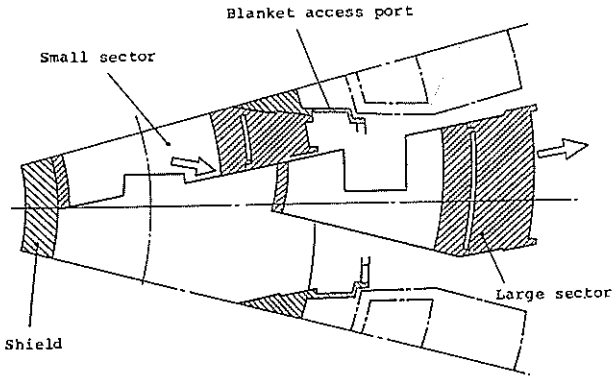

Fig. 3 Two-sector concept with single notion of both sectors

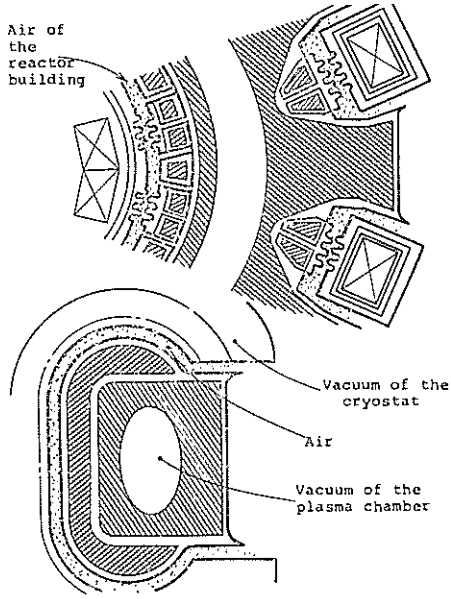

Fig. 4
Simplified separate vacuum boundaries with air in between

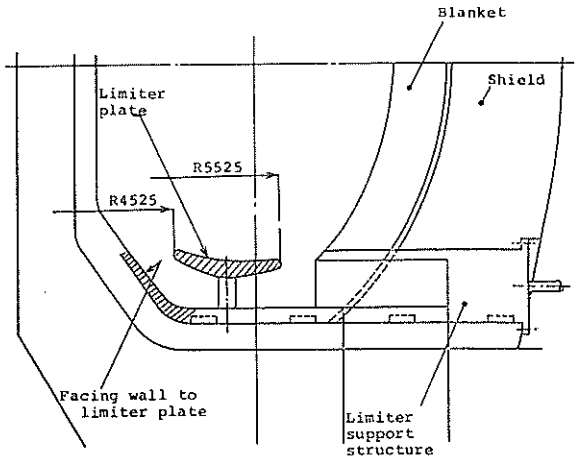

Fig. 5 Replacement region of pumped limiter

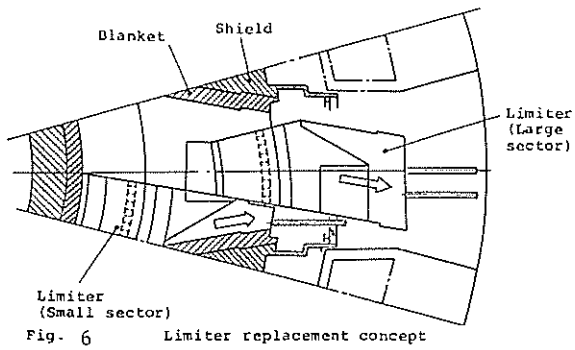

Fig. 6 Limiter replacement concept

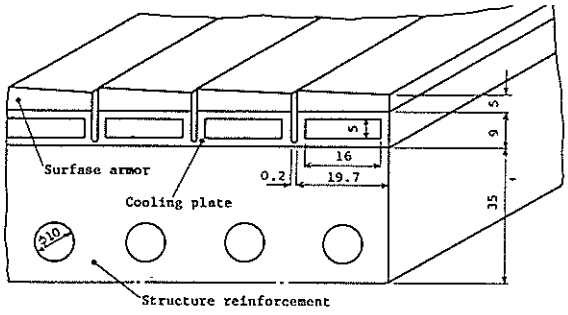

Fig.7 Cross section of brazed limiter plate

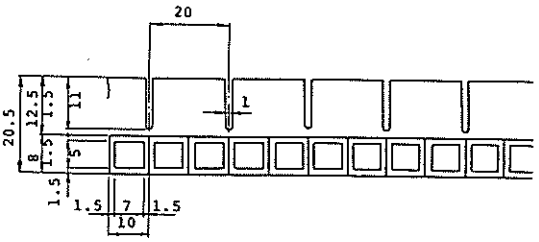

Fig.8 Structure of first wall

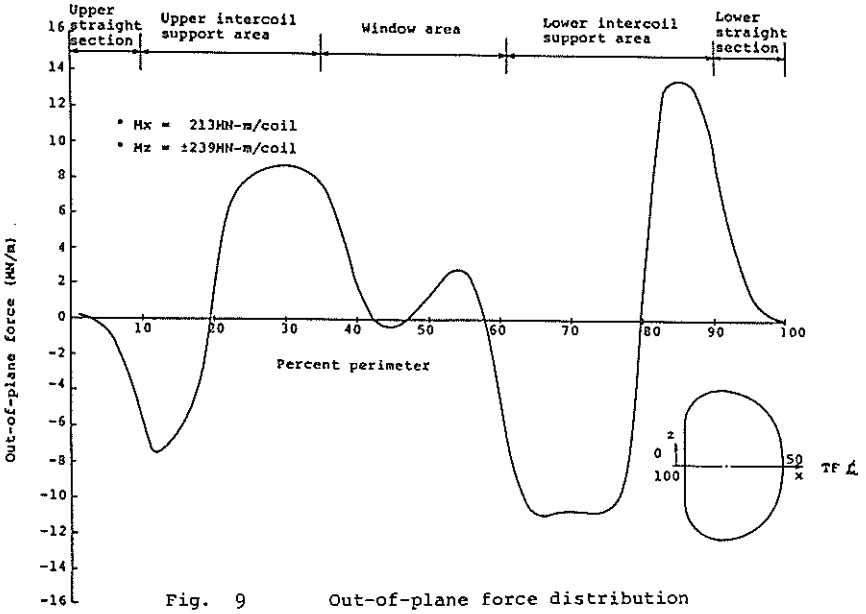

Fig. 9 Out-of-plane force distribution

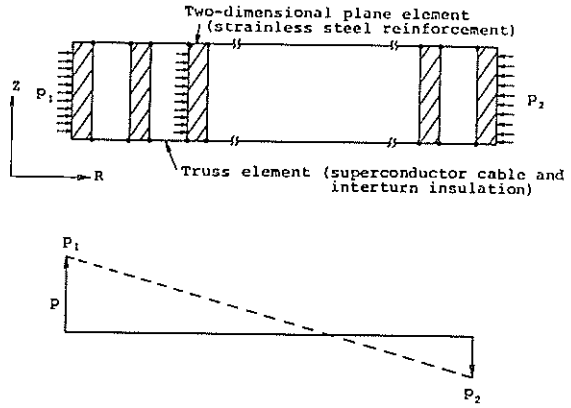

Fig.10 Two-dimensional axisymmetric stress analysis model and loading condition for PF coils

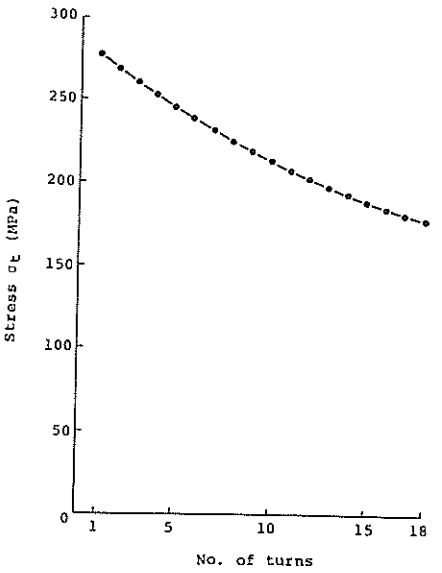

Fig. 11 Stress distribution in radial direction of a central solenoid coil